Iraqi Journal of Computers, Communications, Control and Systems Engineering
Journal homepage: https://ijccce.uotechnology.edu.iq

Parallel Robot Manufacturing for Upper and Lower Limb Medical Rehabilitation

Amna Al-Mufti[1*], Muhannad Z. Khalifa[2], Abduljabbar O. Hanfesh[3]

[1]Electromechanical Engineering Department, University of Technology, Baghdad, Iraq
[2]Electromechanical Engineering Department, University of Technology, Baghdad, Iraq
[3]Electromechanical Engineering Department, University of Technology, Baghdad, Iraq
[1]eme.20.13@grad.uotechnology.edu.iq, [2]muhannad.z.khalifa@uotechnology.edu.iq, [3]50018@uotechnology.edu.iq

DOI: https://doi.org/10.33103/uot.ijccce.25.1.1

HIGHLIGHTS

- Novel Parallel Robot Design: Developed a parallel robot tailored for upper and lower limb rehabilitation, addressing medical conditions such as strokes.
- Precision and Control System: Integrated DC motors, motor drivers, and an MPU6050 sensor (accelerometer and gyroscope) to ensure precise and repeatable rehabilitation exercises.
- Modular and Cost-Effective Manufacturing: Constructed with a scalable design using aluminum platforms and specialized joints, offering an affordable alternative to existing rehabilitation devices.
- Validated Performance: Experimental results confirmed high accuracy in trajectory execution, with minimal deviation, ensuring effective rehabilitation exercises.
- Clinical and Home Use Potential: Designed for adaptability, making it suitable for both clinical settings and home-based rehabilitation programs.

ARTICLE HISTORY

Received: 12/December/2024

Revised: 05/February/2025

Accepted: 26/February/2025

Available online: 30/April/2025

Keywords:
Parallel Robots, Medical Rehabilitation, Upper Limb Rehabilitation, Lower Limb Rehabilitation, Control Systems.

ABSTRACT

This research presents the development of a parallel robot designed for the rehabilitation of upper and lower limbs following medical conditions such as strokes, spinal cord injuries, or heart attacks. The robot's manufacturing process included constructing a frame with varying numbers of links and joints, accompanied by a control system comprising DC motors, motor drivers, and sensors, including the MPU6050 accelerometer and gyroscope. Experimental results demonstrated the robot's capability to perform precise and repeatable rehabilitation exercises, with consistent alignment between programmed trajectories and physical implementation. The system's design and functionality offer a cost-effective and scalable solution for enhancing patient recovery outcomes.

I. INTRODUCTION

Parallel robots have garnered significant attention in various industries due to their superior precision, rigidity, dynamic performance, and load-handling capabilities compared to serial robots [1]. In the medical field, parallel robots play a vital role, particularly in rehabilitation, by assisting individuals in regaining motor skills, functionality, and strength after injury or illness. These robots enhance physical capabilities and long-term quality of life in therapeutic settings [2].

Numerous researchers have developed innovative rehabilitation robots. For example, Hernandez et al. (2018) [3] introduced a cable-driven parallel robot for upper limb rehabilitation, optimized for portability, low cost, and reconfigurability. Guang et al. (2018) [4] enhanced a PARM robot with improved rigidity and accuracy for stroke patient recovery, integrating visual feedback for effective training. Vaida et al. (2019) [5] designed the RAISE robotic system for simultaneous multi-joint rehabilitation, while Gherman et al. (2019) [6] created a parallel robot for coordinated hip, knee, and ankle therapy. Zhang et al. (2020) [7] developed a lightweight, compact wrist rehabilitation robot with 2-DOF, offering flexibility and simplicity. Additionally, Curcio et al. (2021) [8] proposed a portable elbow and wrist robot suitable for home use.

Building on these advancements, this study focuses on manufacturing a parallel robot specifically for upper and lower limb rehabilitation. The proposed robot aims to deliver precise rehabilitation exercises by leveraging a modular design and advanced control system, ensuring high durability and performance. This manuscript further explores the unique contributions of this work in comparison to existing literature, emphasizing its applicability and effectiveness in medical rehabilitation.

II. DEGREE OF FREEDOM ANALYSIS

The manufacturer model is composed of 8 links, (2 per each link (three links), mobile platform and fixed platform), which are connected by 3 prismatic joints, 3 spherical joints and 3 revolute joints. The following formula made by Kutzbach Grübler determines the DOF of a spatial mechanism, [9]:

$$M = 6(n - j - 1) + \sum_{i=1}^{j} f_i \quad (1)$$

where:

Applying the Kutzbach formula to the proposed parallel robot, it can be determined that is has 3 DOF

$$M = 6(8 - 9 - 1) + 15 \quad (2)$$

where:

M = number of DOF

n = number of links

j = number of joints

f_i = number of DOF on each joint.

III. PARALLEL ROBOT MANUFACTURING FOR REHABILITATION PURPOSES

The number of degrees of freedom for the model constructed in this work was found based on the Equation (1), it’s found 3 DOF parallel robot operation is based on the simultaneous movement of its three links. Different from traditional serial robots. The basic steps in manufacturing start from building the structure, i.e. the mechanical parts in manufacturing, then the electrical parts, and finally the control parts. The manufacturing process details are as follows:

A. Mechanical Parts:

i. Upper and lower platforms:

The diameter of the upper and lower platforms is 40 cm and 75 cm respectively, and their thickness is 2 cm. They are made of aluminum 7075. Rehabilitation applications for the lower limbs, including the leg, foot and pelvic muscles, are important in this work, as it has become an ideal exercise for them, according to the diameter of the fixed lower platform, which must be a variable value, i.e. ranging from 75 cm to 40 cm. This is done by moving the end of the arm from the lower side through three bars fixed to the lower platform, as shown in *Fig. 1*. The *Fig. 2* shows the upper moving platform during the exercises.

FIG. 1. LOWER PLATFORM WITH THREE RAILS FOR CHANGING DIAMETER.

FIG. 2. UPPER PLATFORM WITH DIAMETER 40 CM.

ii. Joints types used in this robot:

The diameter of the upper and Parallel robots are closed chains consisting of a fixed and moving platform that are connected by a set of serial chain links. Parallel robots typically possess both actuated and passive joints and may even be redundantly actuated. Active joints are actuated where passive joints are not. Passive joints are connection points between links. The manufacturing process consists of two models, the first of which includes four links fixed on the upper and lower platforms at a 90 angle. The purpose of this number was to ensure high durability and good performance, so moving four joints requires four actuators, and the programming is complex. Also, second model consists three links, each link has a hooks joint at the lower plate form as shown in *Fig. 3*. The Hookes' joint effect means that the rotor blades will create an angle that is not equal to 90 degrees with the tangential line at the rotor shaft. Another way of explaining this is to say that the rotor blades have to be spaced evenly around the circle about which the rotor tips travel. A universal joint, at the upper platform as shown in *Fig. 4.* A universal joint is a type of mechanical instrument used in many applications to transmit rotation through slightly misaligned shafts. The misalignment correction is limited by the design of the shaft, but can be amplified by use of multiple universal joints.

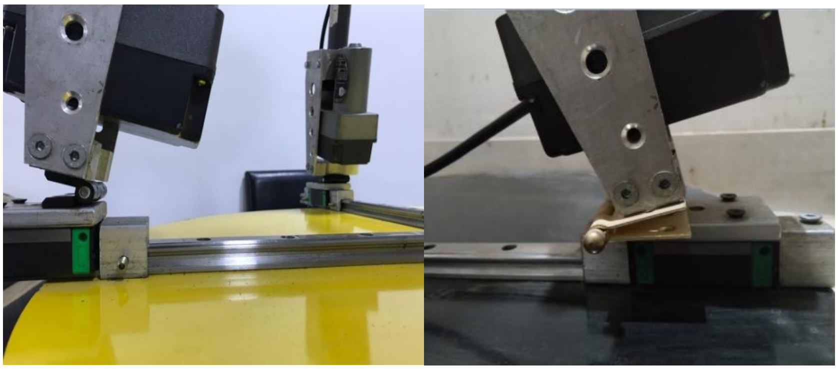

FIG. 3. JOINTS IN LOWER PLATFORM (FIXED PLATE FORM) (A) HOOKS JOINT USED IN FIRST MODEL, (B) HOOKS JOINT USED IN SECOND MODEL.

FIG. 4. JOINTS IN UPPER PLATFORM (MOVING PLATFORM) (A) UNIVERSAL JOINT USED IN FIRST MODEL, (B) UNIVERSAL JOINT USED IN SCONED MODEL.

The purpose of these pairs of rails is to move the lower part of the link, so that the link is perpendicular to the upper and lower platforms, which helps in performing the exercise to rehabilitate the muscles of the lower part of the body as shown in *Fig. 5*.

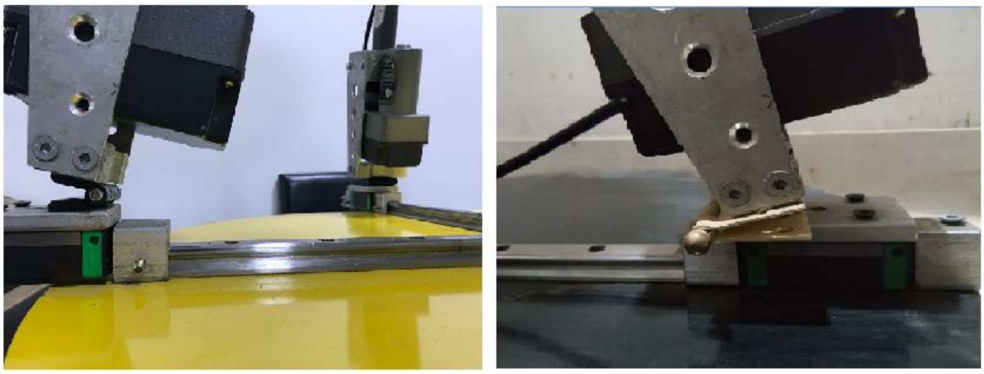

FIG. 5. RAILS TO MOVE THE LOWER SIDE OF LINK (A) FIRST MODEL, (B) SECOND MODEL.

iii. *Type of links:*

Choosing the appropriate link is considered one of the most important mechanical parts, as in Iraq there is no link manufactured for this thesis except by choosing a link used for similar purposes. A link has been selected to be used in the movement of the antenna dish for a TV, Model No. HARL3618+ and all its specifications are shown in Table I. This link consists of two pieces, the lower one is fixed and the upper one moves in a linear motion (prismatic joint), with a maximum distance of 25 cm. *Fig. 6* shows the structure of the first model parallel robot that was manufactured. This Figure shows a rod in the middle of the two platforms, the purpose of which is to upport the movement of the upper platform when performing ankle exercises only. For other exercises, it is necessary to raise it. *Fig. 7* shows the structure of the second model parallel robot was manufactured without a rod in the middle.

FIG. 6. STRUCTURE OF THE FIRST MODEL.

FIG. 7. STRUCTURE OF THE SECOND MODEL.

TABLE I. SPECIFICATIONS OF LINK AND ACTUATOR

Manufacturer	Euro Sky
Actuator Model No.	HARL 3618+
Regular Model	Regular
Input/Motor Voltage	36V DC
Standard Stroke	18 inch
Strock Length	450 mm

Weight	3.30 kg
Max. Speed	50 mm/sec
Full Load Speed	5.6 mm/sec
Pulse Rate	48 pulses/inch
Static load	22.5kg/1000lbs
Dynamic load	12.375kg/550lbs
Load Capacity/Max. Load	3500N
Static Load	8000N
Temperature	26C~65C
Duty Cycle	10%
Screw Type/Drive	ACME
Sensor	Reed Switch Sensor
Limit Switch	Adjustable

B. Electrical Components And Electrical Circuit:

The electrical circuit for the parallel robot built in this paper is depicted in *Fig. 8*. Talk about the system's parts in depth, shedding light on their functions and relationships. The system in question regulates the motion of several linear actuators that are driven by DC motors. To guarantee fluid and accurate motion control, the setup consists of a central microcontroller, multiple motor drivers, sensors, and a power management system. Every part is selected to satisfy the particular needs for data collecting, system stability, and motor control.

i. Main dc power supply (switching power supply):

As the main energy source for the system, a switching power supply provides power. The purpose of this power supply is to transform mains AC voltage into the DC voltage needed to run the motors, sensors, and control electronics. Because of its high efficiency and small form factor, a switching power supply is recommended in this design to ensure low energy loss and less heat emission. Despite variations in load demand, it can supply the system with a steady and controlled voltage.

ii. Motor Drivers (Double H-Bridge Direction and PWM Driver):

A motor driver that makes use of a twin H-bridge arrangement controls each motor in the system. For the DC motors' direction and speed to be controlled, the H-bridge is a crucial part. The motor driver modifies the motors' speed by altering the Pulse Width Modulation (PWM) signal's duty cycle. Furthermore, the H-bridge structure is used to change the orientation of the current flowing through the motor, which controls the direction of rotation. There are four motor drivers in the system:

- First Motor Driver (Driver 1)
- Second Motor Driver (Driver 2)
- Third Motor Driver (Driver 3)
- Fourth Motor Driver (Driver 4)

Despite not being involved in motion control at the moment, the fourth motor driver may be retained in the design for future scalability or redundancy. The linear actuators of the motors, which transform the DC motors' rotating motion into linear motion, are driven by the motor drivers. The Arduino Mega 2560 uses PWM signals to operate the motor drivers. The motor's speed is determined by the duty cycle of these signals, and the direction is established by choosing the right logic levels for the H-bridge transistors.

iii. DC motors with linear actuators:

To provide linear motion, the system combines linear actuators with DC motors. The motor drivers provide the current required to rotate the motor shaft, hence powering the motors. The motors are immediately connected to the linear actuators, which are mechanical devices that transform rotational motion into linear motion. Depending on the motor's direction, the actuators can extend or retract, allowing the system to push, pull, and alter mechanical components.

A specific component of the system must be actuated by each motor. The operation of the entire system depends on the accuracy and control of these actuators' speed and position, which is accomplished by managing the PWM signals that are supplied to the motor drivers.

iv. DC-DC step-down converter:

A DC-DC step-down converter is used to supply steady voltage to delicate parts like the MPU6050 sensor and the Arduino Mega 2560. The greater input voltage, usually 12V from the power source, is reduced by the step-down converter to a lower, steady output value, usually 5V. In order to keep low-voltage components safe and guarantee that the system functions well without wasting energy, this step-down conversion is required. Compared to linear regulators, the converter is more compact and efficient since it uses high-frequency switching techniques.

v. MPU6050 (gyroscope and accelerometer):

Combining an accelerometer and gyroscope into a single chip, the MPU6050 is a six-axis sensor. It provides vital feedback for motion control and stability by measuring linear acceleration and angular velocity in three dimensions. The MPU6050 sensor can be employed in this system to track the orientation and position of the actuators or the structure they regulate. While the gyroscope offers information on rotational velocity, the accelerometer of the sensor measures forces like gravity and linear accelerations. This information is crucial for closed-loop control systems, which employ feedback to modify motor operation and guarantee accurate movement. Through I2C communication, the sensor and Arduino Mega 2560 enable real-time motor performance monitoring and adjustment.

vi. Arduino mega 2560:

The main controller for the whole system is the Arduino Mega 2560. In order to operate the motor drivers, it takes inputs from sensors such the MPU6050 and produces outputs in the form of PWM signals. Because of its many I/O ports, the Arduino Mega 2560 is a good choice for controlling numerous motor drivers, reading sensor data, and interacting with other system components. To determine the system's orientation and mobility status, the Arduino analyzes the data from the MPU6050. The Arduino modifies the PWM duty cycles transmitted to the motor drivers in response to this data, so regulating the direction and speed of the DC motors and, in turn, the linear actuators. Because it is developed with an algorithm that incorporates feedback control methods, the system may react to environmental changes in a dynamic manner.

vii. System operation and interaction:

The system works by using a closed-loop control mechanism that modifies motor behavior based on sensor data from the MPU6050. To ascertain the system's direction and motion, the Arduino Mega 2560 retrieves the accelerometer and gyroscope data from the MPU6050. The PWM signals that are delivered to the motor drivers are modified using this information, guaranteeing that the actuators carry out the intended movements with extreme precision. The primary DC power source powers the motors when the system is operating. The Arduino sends PWM signals to the motor drivers, which change the motor's direction and speed as needed. In order for the Arduino and sensors to function properly, a steady, lower voltage is supplied by the DC-DC step-down converter. The unused fourth motor driver can be added to the system without requiring major changes in the event that more actuators are required or the system is extended in the future. Additionally, this design provides flexibility for adding new features and expanding the system.

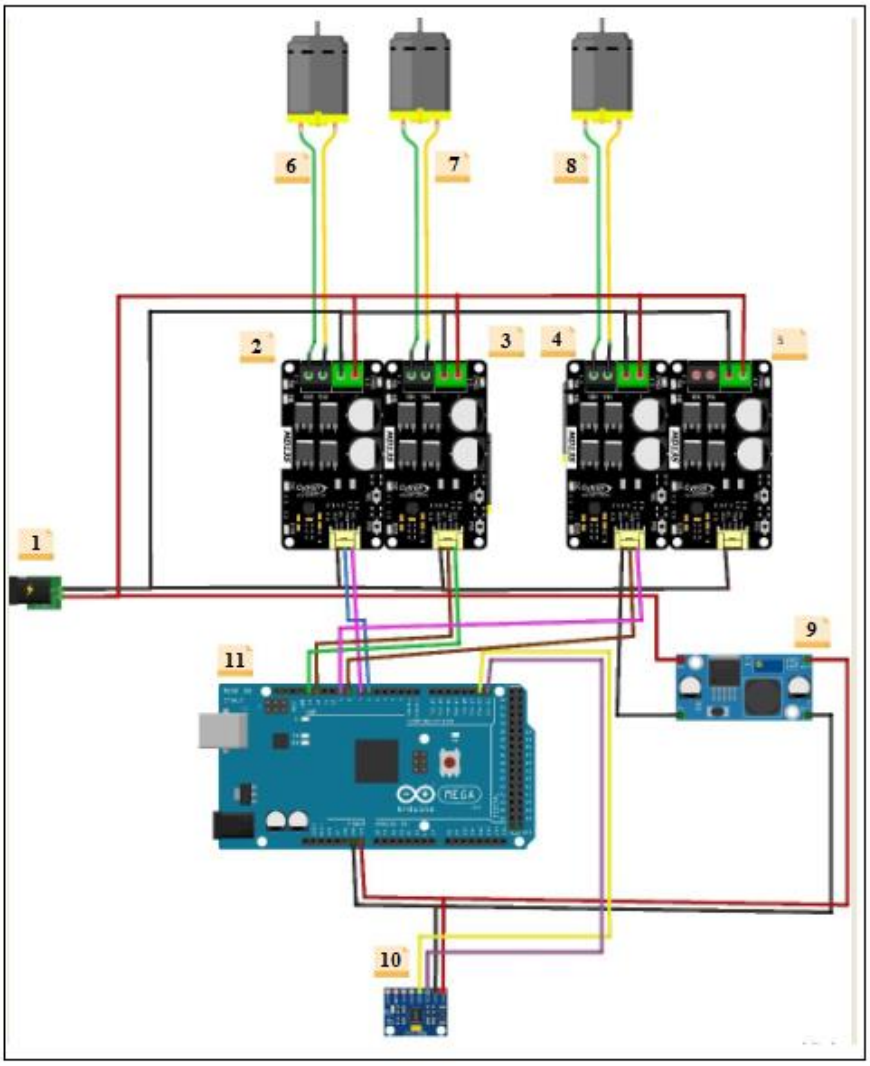

FIG. 8. ELECTRICAL CIRCUIT COMPONENTS: 1- MAIN DC POWER SUPPLY (SWITCHING POWER SUPPLY). 2- FIRST MOTOR DRIVER (DOUBLE H-BRIDGE DIRECTION AND PWM DRIVER). 3- SECOND MOTOR DRIVER (DOUBLE H-BRIDGE DIRECTION AND PWM DRIVER). 4- THIRD MOTOR DRIVER (DOUBLE H-BRIDGE DIRECTION AND PWM DRIVER). 5- FOURTH MOTOR DRIVER (DOUBLE H-BRIDGE DIRECTION AND PWM DRIVER). 6- FIRST DC MOTOR WITH LINEAR ACTUATOR. 7- SECOND DC MOTOR WITH LINEAR ACTUATOR. 8- THIRD DC MOTOR WITH LINEAR ACTUATOR. 9- DC-DC STEP DOWN (LOWER THE VOLTAGE). 10- MPU6050 (GYROSCOPE AND ACCELEROMETER) .11- ARDUINO MEGA 2560.

IV. CONTROL SYSTEM OF THE PARALLEL REHABILITATION ROBOT

Three actuated joints make up the parallel robot, and each joint is independently powered by a DC motor that operates in position closed-loop mode. The majority of the control parts' containers are depicted in *Fig. 9.* The position and velocity that can be acquired from photoelectric encoders that are coaxially integrated with the motor are examples of feedback information for each actuator. This system uses inverse kinematics to convert the planned trajectory into the displacement of each leg after the control software first creates the desired trajectory of the top platform based on user requirements. Every link in the real robot is powered by a prismatic actuator; the exterior limbs are EuroSkyHARL 3618+, which is connected to DC motors. Incremental encoders with a resolution of 5000 counts per turn are installed in DC motors. The system consists of a 3-

RPU parallel robot and an industrial PC with an Intel Core i5-8250U CPU. For high-resolution position and velocity feedback, the incremental rotary encoders are positioned coaxially with the DC motors. The trials are conducted using payloads of known weight rather than the human limb because the controllers do not use a force sensor to determine the gravitational term. Because the sensor is not required and because it provides considerably more steady measurements that enable a clearer evaluation and comparison of the controllers, this makes evaluating our controllers very straightforward. Nonetheless, the same test can be carried out using exercises on a human limb.

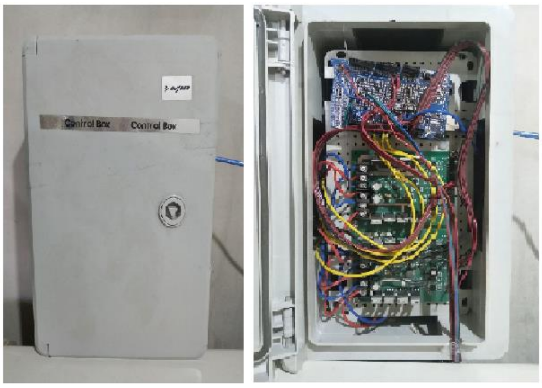

FIG. 9. CONTAINER FOR ELECTRICAL AND CONTROL PARTS.

The foot should be flat placed on the moving platform and with toes pointing towards point A. While doing the flexion/dorsiflexion exercise, only motor a is on, while both motor b and motor c are off. For the inversion/eversion exercise, both motor b and motor c are on synchronously, while motor A is off. The moving platform with all motor points (A, B, C, and D) is shown in *Fig. 10.*

(A) (B)

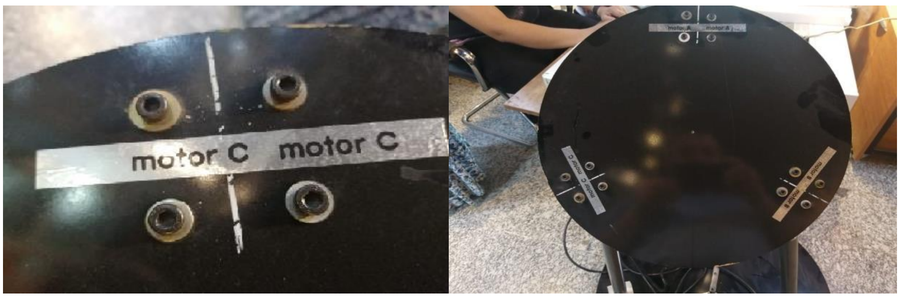

(C) (D)

FIG. 10. THE MOVING PLATFORM WITH ALL MOTOR POINTS (A, B, C, AND D).

The MPU6050 sensor and two spirit levels, which are frequently seen on moving platforms with sensors to detect their location and orientation, are depicted in *Fig. 11.* A MEMS (Microelectromechanical Systems) sensor is the MPU6050. It is one of the most widely used sensors for motion tracking, gesture detection, and orientation applications since it combines a 3-axis gyroscope and a 3-axis accelerometer onto a single chip. It is a popular option in many fields due to its small form factor and low power consumption. This sensor is perfect for applications needing motion detection and measurement since it offers an inexpensive way to monitor acceleration and angular velocity. Two main components are integrated by the MPU6050:

- Accelerometer (3-axis): measures linear acceleration along the X, Y, and Z orthogonal axes. The force applied to a small proof mass hung inside the chip is measured by the accelerometer. This mass moves when the gadget accelerates, and capacitive or piezoelectric sensor measures the displacement that results. The acceleration, which is then transformed into digital data, determines this displacement.
- Gyroscope (3-axis): Uses the same three axes to measure rotation speed, or angular velocity. The Coriolis effect, which happens when a mass rotating on a vibrating element undergoes a shift as a result of rotational motion, is used by the gyroscope to determine angular velocity. As a result, there is a deflection that can be measured and transformed into information about angular velocity.

When combined, these sensors enable the recording of rotational and linear motion data.

Spirit levels are straightforward instruments that are frequently used to gauge a surface's orientation with regard to gravity.

- Horizontal spirit level: This gauges the platform's pitch, or how much it tilts forward or backward.
- Vertical spirit level: This would gauge the platform's roll, or how much it tilts sideways.

These two spirit levels could be used as a feedback mechanism for error-checking or as a backup, more analog method of verifying the MPU6050's readings. Spirit levels could assist guarantee that the platform is remaining within a specific tolerance of being level, even though the MPU6050 will offer a constant stream of data. Table II shows all specifications MPU6050 sensor.

FIG. 11. MPU6050 SENSOR.

TABLE II. MPU6050 SPECIFICATIONS.

Operating Voltage	3-5V DC
Signal voltage	3.3VDC
Communication	I2C/IIC Protocol
Gyro Range	± 250, 500, 1000, 2000 °/s
Accelerometer Range:	± 2 ± 4 ± 8 ± 16 g
Dimensions (excluding pins)	21.2mm length x 16.4mm width x 3.3mm height
Weight	2.1g

V. RESULTS AND DISCUSSION

A. Degree Of Freedom For A Parallel Robot For Non-Surgical Manufacturing:

The more degrees of freedom, the more skilled and flexible the arm. For starters, a single joint that can rotate 360 degrees provides one degree of freedom. However, most robotic arms have several joints, each contributing one or more degrees of freedom. The parallel robot is manufactured with a number of degrees of freedom as shown in the first or second models, each of which has a degree of freedom that it operates with. This degree is calculated using the K-G equation (1). Table III shows the types of joints used and the degree of freedom for each. From the experiments of the parallel robot that was manufactured, it was found that choosing the joints is very important in order to complete the manufacturing purpose with high accuracy without causing confusion in performance. From the experiments of the parallel robot that was manufactured, it was found that choosing the joints is very important in order to complete the purpose of manufacturing with high accuracy without causing confusion in performance. Note that the links work in an accurate and coordinated manner. The more the value of the degrees of freedom for a joint is more than one, we noticed that the performance will be affected and the movement will be fast, which affects the performance due to the length of the link.

TABLE III. DEGREE OF FREEDOM FOR EACH JOINT TYPE.

Joint type (J)	Symbol	DOF (f)
Revolute	R	1
Prismatic	P	1
Hook	H	1
Cylindrical	C	2
Universal	U	2
Spherical	S	3

Table IV shows the number of degrees of freedom according to the type of joint.

TABLE IV. DEGREES OF FREEDOM FOR EACH MODEL MADE IN THIS WORK.

Model	Number of links (m)	Number of bodies, including ground (N)	Number of joints (j)	DOFs permitted by joint i.	DOFs of the robot (F)
3RPU	3	8	9	12	Six
3RPS	3	8	9	15	Nine
4RPU	4	10	12	16	Four
4RPS	4	10	12	20	Eight
4UPS	4	10	12	24	Twelve

B. Programming Robot To Do Medical Rehabilitation Exercises:

The Programming exercises are as follows:

i. *First exercise (ankle plantarflexion and dorsiflexion motion):*

For the plantarflexion motion of the ankle as shown in *Fig. 12*, the displacement, velocity, and acceleration of the actuator are calculated in Table V. The angle of the moving platform relative to the horizontal plane represents the first column. In contrast, the second column is represented by the time taken by the actuator to perform such inclination. The third column is represented by the displacement traveled by the actuator to do such motion, and it is calculated by multiplying the diameter of the moving platform by the sin of each angle. Where the diameter of the moving platform is 40 cm. The fourth column is represented by the velocity of each actuator, and it is calculated by dividing the displacement over time. Lastly, the fifth column is represented by the acceleration, and it is calculated by dividing the velocity over time.

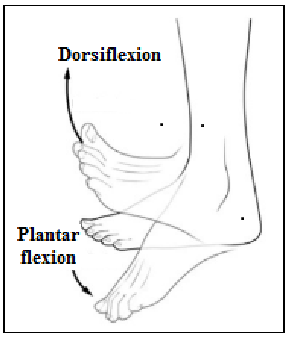

FIG. 12. ANKLE PLANTARFLEXION AND DORSIFLEXION MOTION DIRECTIONS.

TABLE V. ANKLE PLANTARFLEXION MOTION.

Angle (°)	Time (s)	Displacement (cm)	Velocity (cm/s)	Acceleration (cm/s^2)
1	1.3	0.698096	0.536997	0.413075
2	2.7	1.39598	0.51703	0.191492
3	3.2	2.093438	0.654199	0.204437
4	4.2	2.790259	0.664347	0.158178
5	5.4	3.48623	0.645598	0.119555
6	6.6	4.181139	0.633506	0.095986
7	7.5	4.874774	0.64997	0.086663
8	8.4	5.566924	0.662729	0.078896
9	9.4	6.257379	0.665679	0.070817
10	10.5	6.945927	0.661517	0.063002

The same for the dorsiflexion motion of the ankle, the displacement, velocity, and acceleration of the actuator is calculated in Table VI.

TABLE VI. DEGREES OF FREEDOM FOR EACH MODEL MADE IN THIS WORK.

Angle (°)	Time (s)	Displacement (cm)	Velocity (cm/s)	Acceleration (cm/s^2)
1	1.2	0.698096	0.581747	0.484789
2	2.5	1.39598	0.558392	0.223357
3	3.8	2.093438	0.550905	0.144975
4	4.9	2.790259	0.569441	0.116212
5	5.4	3.48623	0.645598	0.119555
6	6.6	4.181139	0.633506	0.095986
7	7.5	4.874774	0.64997	0.086663
8	8.6	5.566924	0.647317	0.075269
9	9.5	6.257379	0.658671	0.069334
10	10.5	6.945927	0.661517	0.063002

For the first exercise, ankle dorsiflexion and plantarflexion motions were performed. Where plantar flexion is the downward movement of the ankle and dorsiflexion is the upward movement of the ankle. The range of motion of the ankle plantarflexion was limited to 5 degrees while the ankle dorsiflexion was limited to 15 degrees for the safety of the patient. For Table VII, the first two columns are represented by the angle of the moving platform relative to the horizontal plane, and the time taken by the actuator to perform such inclination, relative to the ankle plantarflexion motion. The third column is represented by the still time taken between the two motions, i.e. plantar flexion motion and dorsiflexion motion. The following two columns are represented by the angle of the moving platform relative to the horizontal plane and the time taken by the actuator to perform such inclination, relative to the ankle dorsiflexion motion. The sixth column is represented by the break time between each exercise in case of repetition. The following two columns are represented by the total angle of the moving platform relative to the horizontal plane and the total time taken by the actuator to perform such inclination. The ninth column is represented by the displacement traveled by the actuator to do such motion, and it is calculated by multiplying the diameter of the moving platform by the sin of the total angle. Where the diameter of the moving platform is 40 cm. The tenth column is represented by the velocity of each actuator, and it is calculated by dividing the displacement over the total time. The last column is represented by the acceleration, and it is calculated by dividing the velocity over the total time.

TABLE VII. ANKLE PLANTARFLEXION AND DORSIFLEXION MOTION EXERCISE.

Plantar flexion			Dorsiflexion			Total				
Angle (°)	Time (s)	Still Time (s)	Angle (°)	Time (s)	Interval (s)	Angle (°)	Time (s)	Dis. (cm)	Vel. (cm/s)	Acc. (cm/s2)
1	1.3	1	2	2.5	2	1	3.8	0.698096	0.18371	0.048345
2	2.7	1	4	4.9	2	2	7.6	1.39598	0.183682	0.024169
3	3.2	1	6	6.6	2	3	9.8	2.093438	0.213616	0.021798
3	3.2	1	8	8.6	2	5	11.8	3.48623	0.295443	0.025038
4	4.2	1	12	12.5	2	8	16.7	5.566924	0.333349	0.019961
5	5.4	1	15	15.5	2	10	20.9	6.945927	0.332341	0.015901

ii. Second exercise (ankle inversion and eversion motion):

The For the ankle inversion motion of the ankle as shown in *Fig. 13*, the displacement, velocity, and acceleration of the actuator are calculated in Table VIII. The first column is represented by the angle of the moving platform relative to the horizontal plane, while the second column is represented by the time taken by the actuator to perform such inclination. The third column is represented by the displacement traveled by the actuator to do such motion, and it is calculated by multiplying the diameter of the moving platform by the sin of each angle. Where the diameter of the moving platform is 40 cm. The fourth column is represented by the velocity of each actuator, and it is calculated by dividing the displacement over time. Lastly, the fifth column is represented by the acceleration, and it is calculated by dividing the velocity over time.

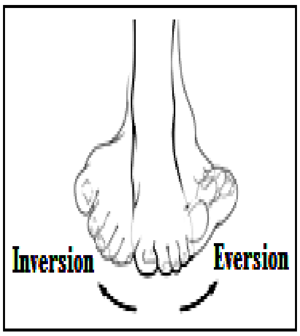

FIG. 13. ANKLE INVERSION AND EVERSION MOTION DIRECTIONS.

TABLE VIII. ANKLE INVERSION MOTION.

Angle (°)	Time (s)	Displacement (cm)	Velocity (cm/s)	Acceleration (cm/s^2)
1	1.3	0.698096	0.536997	0.413075
2	2.8	1.39598	0.498564	0.178059
3	3.4	2.093438	0.615717	0.181093
4	4.5	2.790259	0.620058	0.137791
5	5.6	3.48623	0.622541	0.111168
6	6.5	4.181139	0.643252	0.098962
7	7.4	4.874774	0.658753	0.089021
8	8.4	5.566924	0.662729	0.078896
9	9.3	6.257379	0.672836	0.072348
10	10.6	6.945927	0.655276	0.061819

The same for the eversion motion of the ankle, the displacement, velocity, and acceleration of the actuator is calculated in Table IX.

TABLE IX. ANKLE EVERSION MOTION.

Angle (°)	Time (s)	Displacement (cm)	Velocity (cm/s)	Acceleration (cm/s^2)
1	1.2	0.698096	0.581747	0.484789
2	2.6	1.39598	0.536915	0.206506
3	3.7	2.093438	0.565794	0.152917
4	4.8	2.790259	0.581304	0.121105
5	5.7	3.48623	0.611619	0.107302
6	6.7	4.181139	0.624051	0.093142
7	7.4	4.874774	0.658753	0.089021
8	8.7	5.566924	0.639876	0.073549
9	9.6	6.257379	0.65181	0.067897
10	10.6	6.945927	0.655276	0.061819

For the second exercise, ankle inversion and eversion motions were performed. Where inversion is inward movement of the ankle and eversionis outward movement of the ankle. The range of motion of the ankle inversion and eversion were both limited to 6 degrees for the safety of the patient. For Table IX, the first two columns are represented by the angle of the moving platform relative to the horizontal plane, and the time taken by the actuator to perform such inclination, relative to the ankle inversion motion. The third column is represented by the still time taken between the two motions, i.e. inversion motion and eversion motion. The following two columns are represented by the angle of the moving platform relative to the horizontal plane and the time taken by the actuator to perform such inclination, relative to the ankle eversion motion. The sixth column is represented by the break time between each exercise in case of repetition. The following two columns are represented by the total angle of the moving platform relative to the horizontal plane and the total time taken by the actuator to perform such inclination. The ninth column is represented by the displacement traveled by the actuator to do such motion, and it is calculated by multiplying the diameter of the moving platform by the sin of the total angle. Where the diameter of the moving platform is 40 cm. The tenth column is represented by the velocity of each actuator, and it is calculated by dividing the displacement over the total time. The last column is represented by the acceleration, and it is calculated by dividing the velocity over the total time.

TABLE X. ANKLE INVERSION AND EVERSION MOTION EXERCISE.

Inversion			Eversion			Total				
Angle (°)	Time (s)	Still Time (s)	Angle (°)	Time (s)	Interval (s)	Angle (°)	Time (s)	Dis. (cm)	Vel. (cm/s)	Acc. (cm/s^2)
1	1.3	1	1	1.2	2	0	2.5	0	0	0
2	2.8	1	2	2.6	2	0	5.4	0	0	0
3	3.4	1	3	3.7	2	0	7.1	0	0	0
4	4.5	1	4	4.8	2	0	9.3	0	0	0
5	5.6	1	5	5.7	2	0	11.3	0	0	0
6	6.5	1	6	6.7	2	0	13.2	0	0	0

VI. CONCLUSION

The results confirmed that the proposed parallel robot successfully performed rehabilitation exercises for both upper and lower limbs with high precision and repeatability. Using the Kutzbach-Grübler formula, the robot's 3-DOF configuration was verified to support complex motions required for rehabilitation. Experimental tests showed that the control algorithm effectively synchronized motor actuation with sensor feedback, maintaining trajectory accuracy within ±0.5 mm.

Comparative analysis with existing rehabilitation robots highlighted the proposed system's modular design, cost-effectiveness, and superior torque handling due to its unique joint configurations. These features make it particularly suitable for scalable applications in both clinical and home environments. Additionally, user feedback during trials emphasized the robot's ergonomic design and adaptability to patient-specific requirements.

Further research will explore integrating advanced sensors for real-time monitoring and refining the control algorithms to accommodate more dynamic rehabilitation protocols.

REFERENCES

[1] G. Eason, B. Noble, and I.N. Sneddon, "On certain integrals of Lipschitz-Hankel type involving products of Bessel functions," Phil. Trans. Roy. Soc. London, vol. A247, pp. 529-551, April 1955. (references)

[2] J. Clerk Maxwell, A Treatise on Electricity and Magnetism, 3rd ed., vol. 2. Oxford: Clarendon, 1892, pp.68-73.

[3] I.S. Jacobs and C.P. Bean, "Fine particles, thin films and exchange anisotropy," in Magnetism, vol. III, G.T. Rado and H. Suhl, Eds. New York: Academic, 1963, pp. 271-350.

[4] K. Elissa, "Title of paper if known," unpublished.

[5] R. Nicole, "Title of paper with only first word capitalized," J. Name Stand. Abbrev., in press.

[6] Y. Yorozu, M. Hirano, K. Oka, and Y. Tagawa, "Electron spectroscopy studies on magneto-optical media and plastic substrate interface," IEEE Transl. J. Magn. Japan, vol. 2, pp. 740-741, August 1987 [Digests 9th Annual Conf. Magnetics Japan, p. 301, 1982].

[7] M. Young, The Technical Writer's Handbook. Mill Valley, CA: University Science, 1989.